This is a preprint manuscript of an article that was accepted for publication in April 2017 in the Journal of the American Water Resources Association. The DOI for the final publication is 10.1111/1752-1688.12537.

The Impact of Projected Climate Change Scenarios on Nitrogen Yield at a Regional-Scale for the Contiguous United States

Md Jahangir Alam, Jonathan L. Goodall, Benjamin D. Bowes, and Evan H. Girvetz

Engineer, Ph.D. (Alam), Hazen and Sawyer, Birmingham, AL 35244; Associate Professor, Ph.D. (Goodall), Department of Civil and Environmental Engineering, University of Virginia, 351 McCormick Road, Charlottesville, Virginia 22904; Graduate Student (Bowes), Department of Civil and Environmental Engineering, University of Virginia; Senior Scientist, Ph.D. (Girvetz), International Center for Tropical Agriculture (CIAT), Nairobi, Kenya. (E-mail/Goodall: goodall@virginia.edu)

ABSTRACT

Improved understanding of the potential regional impacts of projected climatic changes on nitrogen yield is needed to inform water resources management throughout the US. The objective of this research is to look broadly at watersheds in the contiguous United States to assess the potential regional impact of changes in precipitation (P) and air temperature (T) on nitrogen yield. The SPARROW model and downscaled P and T outputs from 14 General Circulation Models (GCMs) were used to explore impacts on nitrogen yield. Results of the analysis suggest that projected changes in P and T will decrease nitrogen yield for the majority of the contiguous United States, including the watersheds of the Chesapeake Bay and Gulf of Mexico. Some regions, however, such as the Pacific Northwest and Northern California, are projected to face climatic conditions that, according to the model results, may increase nitrogen yield. Combining the projections of climate-driven changes in nitrogen yield with projected changes in watershed nitrogen inputs could help water resource managers develop regionally-specific, long-term strategies to mitigate nitrogen pollution.

Key Terms: Climate Change; Nitrogen; Regional-scale Environmental Modeling; SPARROW; GIS

INTRODUCTION

During the twentieth century anthropogenic activity has doubled the turnover rate of the global nitrogen (N) cycle (Vitousek *et al.*, 1997; Gruber and Galloway, 2008). The increased availability and input of N, which is a limiting nutrient, to coastal and estuarine waterbodies can lead to eutrophication and the formation of hypoxic dead zones (Diaz and Rosenburg, 2008). These conditions lead to reductions in fish and shellfish production, losses to biotic diversity, harmful algal blooms, and changes in ecological food web structures (Diaz and Rosenburg, 2008; Howarth et al., 2011). Studies suggest that about 20 to 27% of the anthropogenic N input to the landscape is exported to streams and the remaining 75 to 80% is stored or denitrified in the landscape in North American watersheds (Hong *et al*., 2013; Howarth *et al.*, 2006). For the purposes of this study, we call the amount of N delivered to streams and waterbodies from the landscape the N yield (kg/ha yr). The N yield to a stream reach from its subcatchment, without considering upstream contributions, is called incremental N yield (kg/ha yr).

Previous studies have shown that watersheds with higher precipitation (P), runoff, and discharge tend to export a greater fraction of N to streams (Han *et al.*, 2009; Howarth *et al.*, 2012; Kaushal *et al.*, 2008). While a complete understanding of the processes that result in this correlation between wet vs. dry watersheds and N yield is missing, researchers hypothesize that wet watersheds have lower residence times, and therefore there is less time for denitrification processes to occur in the landscape of these watersheds before N inputs are transported to downstream waterbodies (Howarth *et al.*, 2006, 2012). Previous studies have also demonstrated a relationship between air temperature (T) and N yield (Schaefer and Alber, 2007; Seitzinger, 1988; Veraart *et al.*, 2011). These studies have shown that watersheds with higher T tend to have lower N yields, possibly due to a higher rate of denitrification in the landscape of these watersheds (Schaefer and Alber, 2007). In addition, in shallow waters, higher T tends to decrease solubility of oxygen and increase respiration, resulting in a synergistic effect that boosts denitrification (Veraart *et al.*, 2011). With P and T at odds in terms of their impact on N yield, the potential impact of climate change on N yield remains uncertain (Najjar *et al.*, 2010).

Part of the challenge in understanding climate change impacts on N yield is determining the role of storage of N in terrestrial pools in controlling the observed difference between N yield in wet and dry years. During dry years, N accumulates in the landscape due to reduced hydrologic transport and uptake by plants through transpiration. During wet years, this store of terrestrial N is flushed to streams (Davis *et al*., 2014; Goolsby *et al.*, 1999; McIsaac *et al*., 2016; Van Meter *et al*., 2016). Given this, one might conclude that there would be no significant long term impact of climate change on average N yield because there is a steady-state rate at which N is stored and then flushed from the landscape. However, Sinha and Michalak (2016), using a long term data set of Net Anthropogenic Nitrogen Inputs (NANI), land use, and P as model inputs, showed that changes in P are significant in controlling the interannual variability of N loading across large spatial scales. Likewise, Howarth *et al*. (2012) showed using a large database of N yield data in the United States and Europe that climate is correlated with N yield. Thus, the authors conclude climate change will likely impact N yield and loadings to already stressed waterbodies. The question remains, however, as to the specific regional patterns of impact on N yield due to projected changes in climatic conditions over the coming century.

The objective of this study is to provide insight into the potential impact of projected climate conditions on N yield for different regions in the contiguous United States. We use the SPAtially Referenced Regression On Watershed attributes (SPARROW) model (Schwarz et al., 2006; Smith *et al.*, 1997) to understand the relationship between current P and T conditions and N yield for watersheds in the contiguous United States. SPARROW is a widely used and well-evaluated model appropriate for continental-scale analysis of terrestrial N transport (Schwarz *et al.*, 2006). The model uses mass balance principles and a simplified first-order-decay representation of mass loss due to terrestrial and riverine N transport within a statistical framework for fitting model coefficients. We calibrate our model based on two emission scenarios for 14 general circulation models and baseline conditions in 1992. The model was verified using observed data in 2001 and then used to determine projected N yield change (%) for future time periods, as detailed in the Results and Discussion.

MATERIALS AND METHODS

Model Description

SPARROW is a non-linear regression, process-based water quality model used to predict N loading in unmonitored reaches under long-term, steady-state conditions (Schwarz *et al.*, 2006). SPARROW relates the dependent variable, observed loadings, with the independent variables waterbody/river properties, watershed attributes, and N sources. SPARROW includes reduced-complexity process representations for describing land-to-water, in-stream, and in-reservoir transport. Results from past SPARROW applications suggest these representations are appropriate at the watershed-scale for modeling long-term average conditions across large regions including continental-scale studies (Alexander *et al.*, 2002; Grizzetti *et al.*, 2005).

SPARROW estimates mean annual total N loading at reach *i* as

$$L_i = \left[\left\{ \sum_{j \in J(i)} L_j \right\} A\left(Z_i^s, Z_i^r; \kappa_s, \kappa_r\right) + \left\{ \sum_{n=1}^{N} s_{n,i} \beta_n \right\} D_n\left(Z_i^D; \alpha\right) A'\left(Z_i^s, Z_i^r; \kappa_s, \kappa_r\right) \right] \varepsilon_i \quad (1)$$

where the first term of the equation represents the flux contribution to reach *i* from the adjacent upstream reach and L_j is the flux that exits the adjacent upstream reach. The function *A(.)* represents the instream transport loss. The vectors Z_i^s and Z_i^r represent stream and reservoir characteristics, while κ_s and κ_r represent the stream and reservoir coefficient vectors. The second term of the equation represents the flux that originates in the watershed of reach *i*. The term $s_{n,i}$ represents the contribution from N source *n* to reach *i*. The term β_n is a regression coefficient estimated by the model for source *n*. The function *D(.)* in the equation represents the land-to-water transport process. The vector Z_i^D represents watershed attributes and α is the estimated coefficient for vector Z_i^D. The vector *A′(.)* represents the instream transport loss and ε_i is the multiplicative error term defined by the model (Schwarz *et al.*, 2006).

The function *D(.)* in the SPARROW model equation provided in the paper describes the land-to-water delivery process and is modeled as

$$D_n\left(Z_i^D; \alpha\right) = exp\left(-\alpha' Z_i^D\right) \quad (2)$$

where α' is the vector of the model coefficients that describe the land-to-water delivery for the watershed attribute vector, Z_i^D. The vector $A'(.)$ that represents the instream transport loss is modeled as

$$A\left(Z_i^s, Z_i^r; \kappa_s, \kappa_r\right) = exp\left(-\kappa_s^{'} T_{i,j}\right) \quad (3)$$

where $\kappa_s^{'}$ represents the vector of decay coefficients that is based on the mean annual flow rates of the streams and are estimated as mass loss per unit length of streams. The term $T_{i,j}$ is the vector of waterbody properties including mean annual flow rates. Finally, losses due to lakes or reservoirs is modeled as

$$A\left(Z_i^s, Z_i^r; \kappa_s, \kappa_r\right) = \left(1 + \kappa_r / q_i^r\right)^{-1} \quad (4)$$

where κ_r represents the reservoir decay coefficient and q_i^r is the areal hydraulic loading which is the ratio of reservoir outflow to surface area, in units of distance per time.

The model is implemented in the SAS statistical language and available as an open-source software from the United States Geological Survey (USGS). We used version 2.9 of the SPARROW model, the latest version of the model available when the majority of the modeling work was performed (2011-2013). Additional detail on the SPARROW model including availability of the model code is available from https://water.usgs.gov/nawqa/sparrow/.

Data Preparation

Watershed Attributes and Nitrogen Sources. We used the 1:500,000 spatial scale Enhanced River Reach File 1 (ERF1) dataset (Nolan *et al.*, 2002) for this study as the digital representation of rivers in the contiguous United States. This dataset includes more than 60,000 reaches with estimates of mean streamflow, stream velocity, time of travel, drainage density, mean water depth, and areal hydraulic load. Nitrogen sources in this study are consistent with past SPARROW applications and include fertilizer application, livestock waste, population related sources, atmospheric deposition and nonagricultural non-point source pollution. Consistent with prior studies, we used the watershed level atmospheric deposition data averaged over the period 1991 to 1993, where atmospheric deposition was considered as the wet deposition of inorganic N (nitrate and ammonia) (kg/yr) (Alam and Goodall, 2012; NADP, 2010).

Watersheds for each ERF1 reach were derived from the Hydro1K Digital Elevation Model (U.S. Geological Survey, 2004) using terrain processing algorithms. The National Land Cover Dataset (NLCD) 1992/2001 Retrofit Land Cover Change Product was used to estimate 1992 land use conditions, because using the 1992 NLCD product directly does not make use of the improved land cover/use classification scheme used for the 1992/2001 change product. Average depth-weighted permeability was computed from the State Soil Geographic (STATSGO) database through prior work for each watershed in the model. Human population estimates were used as a surrogate for point sources as population is highly related to the urban wastewater effluent and municipal waste production. County level population estimates were obtained from the United States Census Bureau for 1992. These county level population estimates were then distributed among the watersheds based on their area of urban land use. County level fertilizer application was estimated as both farm and nonfarm fertilizer application. This county level fertilizer application was then distributed among the watersheds based on their amount of crop and urban land using the assumption that fertilizer is applied to both cropland and urban land (as fertilizer for lawns and landscaping). Ruddy *et al*. (2006)

presented a county-level N input dataset of livestock waste for the period 1982-2001. This county level livestock waste dataset considered confined and unconfined manure and was distributed among the watersheds based on their amount of agricultural land. Finally, nonagricultural land in this study was estimated as the sum of only the urban, forest, and grassland. Further detail on the methods for estimating the watershed attributes is provided in Alam and Goodall (2012).

Precipitation and Temperature Changes. The General Circulation Models (GCMs) used in this study are from the World Climate Research Programme's (WCRP's) Coupled Model Intercomparison Project Phase 3 (CMIP3) multi-model dataset (Meehl *et al.*, 2007). We used an ensemble of 14 GCMs for the climate predictions similar to prior studies looking at the impact of climate change on water resources (Brekke *et al.*, 2008; Maurer *et al.*, 2007; Pierce *et al.*, 2009; Reichler and Kim, 2008) (See Table 1 for a list of the GCMs used). The data were statistically downscaled to 1/8º grid cells (approximately 12 by 12 km) and bias-corrected using the approach described by Maurer *et al.* (2007). In this study we considered the two extreme emission scenarios: higher (A2) and lower (B1) future emission scenarios. We refer to model runs for specific times in later sections, but these are in fact averages of multiyear periods where "baseline" or "1992" refers to 1982-2001, "2030" refers to 2020-2039, "2050" refers to 2040-2059, and "2090" refers to 2080-2099. Using a twenty-year averaging window addresses the challenge of inter-annual storage of N in terrestrial pools by looking at longer periods where changes in terrestrial storage between analysis periods should be less.

[INSERT TABLE 1 HERE]

All GCMs used for this work have been previously used in various assessments of the Intergovernmental Panel on Climate Change (IPCC) Fourth Assessment Report and at the time this work was done, output from the third phase of the Coupled Model Intercomparison Project (CMIP3) was the only dataset available for the contiguous U.S. with downscaled resolution as fine as 1/8º. Recent studies comparing CMIP3 with the now available CMIP5 have found only small differences in magnitude and spatial distribution of model outputs including precipitation (Baker and Huang, 2014; Sun *et al*., 2015). Therefore it is expected that the results for this study will be consistent with any results determined using the more updated CMIP5. The GCM outputs are available for different emission scenarios where each scenario represents a different assumption for future human activity, greenhouse gas emission, technology development, and economic growth. The decision to use a twenty-year averaging period around the target year was done in part to reduce the variability in annual P and T projections and to provide long-term conditions for the SPARROW model. The resulting datasets for future P and T for the study area are the average across the 14 downscaled GCM outputs for presentation purposes.

Future projections for both P and T show strong spatial and temporal patterns. T is consistently higher for the contiguous US for all time periods and emissions scenarios (Figure 1). The higher emissions scenario (A2) and longer time horizon produces the greatest T increases, and the Great Plains and mid-western parts of the contiguous US are projected to experience the greatest T increases. While some of the GCMs predict an overall increase in P, others predict a decrease (Figure 2). However, there is general agreement among the model projections for increasing P in most of the contiguous US, with P decreasing in the Great Plains and parts of the southern US.

[INSERT FIGURE 1 HERE]

[INSERT FIGURE 2 HERE]

Establishing Baseline Nitrogen Yield Conditions

SPARROW was first run to establish baseline conditions for N yield (Figure 3). For consistency with projections of future conditions, this model run made use of P and T datasets from the 14 GCMs averaged over a 20-year period around 1992. We did this for both the A2 and B1 emission scenarios, which are nearly identical but have slight differences that are presumably due to underlying assumptions in the emission scenarios. Regression coefficients in the SPARROW model were determined using observed stream discharge and total N concentration data from 354 United States Geological Survey (USGS) National Stream Quality Accounting Network (NASQAN) stations for the period 1970-2000 (Deacon *et al*., 2015). Total N observations were taken as the sum of nitrate, nitrite, and total Kjeldahl N in unfiltered samples. These discharge and concentration data were used to estimate total N loading detrended to 1992, the dependent variable in the SPARROW model, using the FluxMaster model (Schwarz *et al.*, 2006). Detrending the data allowed the analysis to focus on fluctuations in the data and not its overall trend. Additional details on detrending discharge and concentration data can be found in Alam and Goodall (2012).

[INSERT FIGURE 3 HERE]

Modeling the Impact of Future P and T on Incremental N Yield

In order to determine differences in N yield from the baseline model run to future P and T conditions, we assumed the correlations found in the baseline model would hold for future changes in P and T. Average P and T conditions for each watershed in the model were determined by averaging across 20-year time periods centered on the years 2030, 2050, and 2090. We did this so that each watershed has estimates of P and T for the three future time periods based on each of the 14 GCM projections run under two emissions scenarios (A2 and B1). Differences in N yield from the base year (1992) to future conditions (e.g., 2030, 2050 and 2090) were quantified for each watershed in the contiguous United States by applying the SPARROW model. We then spatially aggregated the model results to major river basins to determine regional patterns.

Due to the complexity of modeling continental-scale N transport, we had to make simplifying assumptions in our modeling work. We assumed that over the 20 year averaging periods used in the analysis, terrestrial N storage within watersheds would be constant. SPARROW is a steady-state model used to predict average N transport across regions over long (multiple decade) time periods. Thus the model assumes no change in terrestrial N storage. While there is work to create a seasonally-dynamic version of SPARROW (Smith *et al*., 2013) that incorporates modeling storage changes, a dynamic version of the SPARROW model has not been publically released. For this reason, we used a 20 year averaging period and assumed there will be no significant net change in terrestrial N storage within watersheds over this period. Howden *et al*. (2011) provides support for this assumption by suggesting that at least a 12 year period is necessary to isolate trends in fluvial water chemistry from hydrologic variability.

Another assumption behind the analysis is that the SPARROW regression coefficients will hold into the late century. We calibrated the model coefficients for the baseline conditions in 1992 model to predict N flux for an observed period with sufficient water quality and continental-scale land use data. We used the calibrated model coefficients to predict 2001 conditions and found a good match between observed and modeled conditions, as described in the Results and Discussion section. We also compared our calibrated model coefficients to calibrated model coefficients obtained through past SPARROW studies to test their consistency. In a conversation with SPARROW model developers, it was suggested that another way of considering this assumption is as a "space-for-time substitution (SFT)" (Pickett, 1989). The SFT assumption is that observed correlations between measured watershed properties and N loadings for the set of spatially distributed watersheds within our study region that experience a wide range of P and T conditions inform how changes in future P and T conditions may impact future N yield for these watersheds. This assumption has been used in ecological studies as a method for forecasting the potential impact of future climatic conditions (Blois *et al*., 2013), and shares similarities to the approach used here for looking at a large collection of watersheds to project possible climate change impacts.

RESULTS and DISCUSSION

Model Calibration and Verification

The calibrated baseline (1992) model was able to explain more than 80% of the variability in the observed N loading time series from 354 NASQAN stations for the 1970-2000 time period. For both the A2 and B1 scenarios, the r^2 value for the predicted vs. actual log of flux was 0.89 (Figure 4) and predicted vs actual log of yield was 0.81. The Root Mean Square Error (RMSE) for both the A2 and B1 scenarios was 0.62. The β coefficients were the source coefficients and provide information about the relationship between the sources and the instream N (Table 2). All the β coefficients were statistically significant ($p < 0.05$) except for the livestock waste. The α coefficients, which relate to land-to-water transport and therefore N yield, were statistically significant ($p < 0.05$) except for the drainage density. Instream loss coefficients (κ) for both the low-flow streams ($Q < 28.3$ m^3/s) and medium-flow streams (28.3 m^3/s $\leq Q \leq$ 283 m^3/s) were statistically significant. Higher in-stream loss rates for the small streams is consistent with previous studies using SPARROW (Alexander *et al.*, 2000). Finally, reservoir loss coefficients (κ_r) were also found to be statistically significant in the model calibration.

[INSERT FIGURE 4 HERE]

[INSERT TABLE 2 HERE]

Model Evaluation

In order to evaluate the baseline model performance, the calibrated model was applied to a new time period where sufficient land use and water quality observation data was available (2001). It was found that the model coefficients performed well at explaining observed variation in the 2001 flux dataset; the r^2 value was 0.90 (Figure 5). We also looked at past SPARROW studies and found that our baseline model resulted in calibrated parameters that are similar to those reported in other studies (Alam and Goodall, 2012; Alexander *et al*., 2008; Brown *et al*., 2011; Hoos and McMahon, 2009; Moore *et al*., 2011; Najjar *et al*., 2010; Rebich *et al*., 2011; Robertson and Saad, 2011; Smith *et al*., 1997; Wise and Johnson, 2011). Based on these past studies we found a consistent negative relationship between N loading and mean annual T and a positive relationship between N loading and mean annual P.

[INSERT FIGURE 5 HERE]

Impact of P and T on Incremental N Yield

Differences in incremental N yield from baseline (1992) conditions to future periods (2030, 2050, and 2090) were estimated from an ensemble of 14 SPARROW model runs with different P and T inputs, constructed from the individual GCMs under the A2 and B1 emission scenarios (Figure 6). Incremental N yield considers only the N yield to a stream from its sub-catchment and not upstream contributions. The estimates indicate that changes in P and T conditions will decrease incremental N yield for the vast majority of the study area under both the A2 and B1 emission scenarios. The regions projected to experience the largest increase in T and the largest decrease in P are those where conditions are most conducive to lowering incremental N yield. On the other hand, regions projected to face increased P and a relatively lower increase in T could potentially have higher incremental N yield.

[INSERT FIGURE 6 HERE]

There is significant uncertainty in future P & T conditions caused both by (i) different emission scenarios and (ii) differences across individual models within the ensemble of 14 GCMs used in the analysis. For the A2 (higher emissions) scenario, results suggest an average decrease of 4.4% in incremental N yield by 2030 with a range between no change and a 12% decrease when only P and T are varied and all other model variables are held constant. By the year 2050, the decrease in incremental N yield from baseline conditions for the A2 scenario is about 8.4% on average with a range of 2.2% to 20%. By 2090, the decrease in incremental N yield from baseline conditions using the A2 scenario is projected to be 20% with a range of 4.4% to 38% across the GCMs. For the B1 (lower emissions) scenario, estimates are still for a decrease in incremental N yield from the baseline conditions on average across the study region. These changes in incremental N yield are as follows: by 2030 a 4.6% decrease on average ranging from a 1.57% increase to a 12% decrease; by 2050 a 6.6% decrease with a range of 0.5% to 15%, and by 2090 an 11.5% decrease with a range of 0.6% to 20%. Clearly the uncertainty in this analysis is large. However, the average values across the ensemble of GCMs do suggest that the net effect of P and T changes on incremental N yield, when all other variables are held constant, would be to decrease incremental N yield for the vast majority of the contiguous United States.

There are underlying mechanistic processes that provide support for the observed correlations between T, P, and N yield. As we discussed earlier, increases in T are thought to aid in denitrification processes (Seitzinger, 1988; Veraart *et al*., 2011) by lowering the amount of reduced N and decreasing N yield. Decreases in P produce longer residence time in dry conditions and increase N retention by the soil, plants, and microbes (Howarth *et al*., 2006). Increased P can increase runoff and cause greater transport of N from the landscape to streams and waterbodies (Nangia *et al*., 2010). Heavily fertilized river basins like the Mississippi can be more sensitive to P; a small increase in P can lead to a large increase in N loading (Donner and Kucharik, 2003). During wet years, not only does N yield from land increase, but the instream N removal also decreases and leads to a large increase in N loading to the stream (Donner and Kucharik, 2004). A study of a semiarid Arizona watershed using the physically-based SWAT model suggested a decrease in nitrate export due to a projected warmer and drier climate (Ye and Grimm, 2013). For these reasons, we argue that it is reasonable to assume that the correlations found by the SPARROW for the baseline model have some predictive power for observed periods, consistency across a variety of study areas, and are in line with known mechanistic relationships between T, P, and N yield.

Assessment of Regional Patterns

Incremental N yield results and comparisons from the baseline period to the periods 2030, 2050, and 2090 are summarized and presented for hydrologic regions (2-

digit HUC) for the contiguous United States (Figure 7). Names and numbers for the hydrologic regions are provided in Figure 8 and Table 3. The model results suggest incremental N yield, when considering changes in P and T and holding all other variables constant, will decrease most significantly in the Arkansas-White-Red, Texas-Gulf, Rio Grande, and Upper Colorado regions due to changes in P and T. The average decrease for these regions is 7% by 2030 based on both the A2 and B1 scenarios. By 2050, these regions would have an average incremental N yield decrease of about 13% based on the A2 scenario and 9% based on the B1 scenario,. By the year 2090, the highest average decrease would be about 25% based on the A2 scenario and 15% based on the B1 scenario. Regions with the lowest decrease across both scenarios and time periods include New England, South Atlantic-Gulf, and Mid-Atlantic.

While regional averages point to decreases in incremental N yield from projected changes in P and T, there are watersheds within these regions where the results suggest that future P and T conditions may increase N yield from baseline conditions. These watersheds are located throughout the study region, as indicated by the whiskers in the plots given in Figure 7. Figure 6 shows clusters of these watersheds appearing in the Pacific Northwest and Northern California. Projected changes in N yield in these regions due to changes in P and T are as high as 15% by 2050 and 25% by 2090. These regions tend to have more moderate projected increases in T and higher projected increases in P compared to other watersheds within the study area. Plans to reduce N pollution within waterbodies impacted by these watersheds in particular should incorporate projected climate change impacts.

[INSERT FIGURE 7 HERE]

[INSERT FIGURE 8 HERE]

[INSERT TABLE 3 HERE]

Consequences of Regional Patterns for Impaired Waterbodies

The results of this study have management implications for waterbodies in the contiguous US, such as the Chesapeake Bay (Kemp, *et al*., 2005) and the Gulf of Mexico (Diaz and Rosenberg, 2008), where nutrient pollution, eutrophication, and hypoxia are major concerns. Based on the modeling results, subcatchments in the Chesapeake Bay Watershed, considered here as the Mid-Atlantic Region (02), will have a median decrease in incremental N yield of 3.6%, 4.4%, and 13.9% in the 2030, 2050, and 2090 time periods, respectively, for the A2 emission scenario. The B1 emission scenario shows median N yield decreases of 3.4%, 4.8%, and 9.0% for the same time periods. The Gulf of Mexico's watershed also shows median decreases in incremental N yield in both emission scenarios and through all three study periods. Regions impacting the Gulf of Mexico include the South Atlantic-Gulf (03), Ohio (05), Tennessee (06), Upper Mississippi (07), Lower Mississippi (08), Missouri (10), Arkansas-White-Red (11), and Texas-Gulf, (12), which are parts of the Mississippi-Atchafalaya River Basin. The average of the median decreases in incremental N yield for these regions are 5.4%, 8.7%, and 19.8% based on the A2 scenario, and 5.2%, 6.9%, and 11.7% based on the B1 scenario, for the corresponding time periods of 2030, 2050, and 2090. These results are based solely on changes to P and T. However, combining the projections of climate-driven changes in N yield with projected changes in watershed N inputs could help water resource managers develop regionally-specific, long-term strategies to mitigate N pollution in heavily impaired waterbodies.

Comparison of Model Results with Prior Studies

A limited number of previous studies have used GCMs to project estimates of climate change impacts on N yield. Howarth, *et al*. (2006), in one of the early studies exploring this topic, used GCM predicted P and discharge values to estimate future discharge and subsequent N export from the Susquehanna River to the Chesapeake Bay. They reported a mean change in P from baseline study values of +4% by 2030 and +15% by 2095. The reported mean change in discharge is +2% by 2030 and +11% by 2095. They found that these changes in P and discharge corresponded with a change in riverine N flux ranging from +3% to +17% and +16 to +65% by 2030 and 2095, respectively. The authors noted that N responds nonlinearly to climate changes; a small change in precipitation can cause a large change in N flux. However, by basing the change in riverine N flux only on P and discharge, the authors miss the effect that projected increases in T can have on lowering N flux. Incorporating T in our model, as well as using an ensemble of 14 GCMs, resulted in decreasing projected N yield for much of the Susquehanna River Basin.

More recently, the Soil and Water Assessment Tool (SWAT) hydrologic model has been used with GCM outputs in several studies at varying spatial scales. For a 505 km^2, semi-arid Arizona watershed within the Lower Colorado region, Ye and Grimm (2013) predicted a decrease in N export, over the current mean value of 30 kg N day^{-1}, of 33%, 50%, and 60% by the 2020s, 2050s, and 2080s, respectively. Our results for the

Lower Colorado region, which includes the watershed studied by Ye and Grimm (2013), indicate an average incremental N yield decrease in the A2 emission scenario of 6%, 10%, and 23% and in the B1 scenario of 4%, 9%, and 16% for the respective time periods of 2030, 2050, and 2090.

Two studies of the Upper Mississippi River Basin (UMRB) also made use of a SWAT-GCM coupling. The UMRB, with its large amount of agricultural land, contributes to nutrient pollution of the Gulf of Mexico. To model this region, Jha, *et al*. (2015) showed N yield change based on a SWAT-GCM coupling of projected P and T at the subcatchment level. They found that subcatchments in the UMRB with higher P for the mid-century (2046-2065) had increased N yield; increased T in subcatchments with minimal changes in P showed decreased N yield. Roughly half of the subwatersheds in Iowa showed decreases in N yield, while all of the UMRB subwatersheds in Illinois showed increases in N yield. The study highlighted that future climate can increase water quality problems in some subwatersheds, while causing improved water quality in others. Their overall predicted change in average annual nitrate-N loading patterns for the UMRB ranged from -38% to +101% with an average increase of 13% over the entire basin (based on the average nitrate+nitrite value in Figure 6 from Jha, *et al*., (2006)). Panagopoulos, *et al.* (2014), while exploring the impact of agricultural practices on nutrient export under current and projected climate conditions, showed a decrease in N export from the UMRB over their modeled 1981 to 2000 baseline. Based on a single GCM projection, they predicted decreases of 13% in nitrate-N and 17% in total N by 2046-2065. Our results for the Upper Mississippi region projected decreases in median incremental N yield of 5.4%, 7.1%, and 17.8% for the A2 scenario and 4.4%, 6.2%, and 11.0% for the B1 scenario for the respective 2030, 2050, and 2090 time periods.

Variability Across Watersheds Under Two Emission Scenarios

The model results can be summarized by the relationship between average change in T (°C), P (mm), and incremental N yield change from baseline conditions (%) for the two emission scenarios (Figure 9). This was done for all 14 GCMs for both the A2 and B1 emission scenarios and averaged for the 2,149 USGS 8-digit cataloging unit (Seaber *et al.*, 1987) watersheds. The boxed clusters of points in the two subplots are results for the three time periods used in the analysis (2030, 2050, and 2090), with each point representing an individual watershed. The variability in T and P can be seen clearly in Figure 9. The higher emissions in the A2 scenario led to greater projected changes in T and P, causing the larger distribution of points. With lower emissions in the B1 scenario, there is less projected change in T and P, which causes the denser clustering of points. Figure 9 provides valuable insights into P and T changes and how these changes impact incremental N yield for the collection of watersheds in the contiguous US. While T shows a clear upward trend for the majority of the watersheds, P does not. The majority of watersheds do show an increase in P, but many show a decrease in P. There are clear demarcations in the plot at which a given change in P and T will result in a certain N yield change. While most watersheds fall inside of these zones, there are individual watersheds that have different N yield changes than the surrounding watersheds with the same T and P changes. This indicates that N yield change in these watersheds is more heavily influenced by other factors, such as a major point source or high urbanization, than by changes in T and P. These results provide useful information to water resource managers by showing expected changes in incremental N yield for a given change in P and T for most watersheds, but also the potential for outlier watersheds with unique properties resulting in atypical changes in incremental N yield.

[INSERT FIGURE 9 HERE]

CONCLUSIONS

The goal of this study is to improve understanding of regional changes in N yield that may result from projected long term changes in P and T. The SPARROW model offers a means for gaining insight into how watershed characteristics, including average P and T, result in N transport including N yield. We used SPARROW and future projections of P and T from across an ensemble of 14 GCM models for two different emission scenarios to identify how projected regional patterns in P and T might influence future regional patterns in N yield.

The results suggest that projected climatic conditions may decrease N yield from the landscape to waterbodies for the majority of the contiguous US. Increases in T, which are thought to lower N yield by increasing denitrification processes, will often outweigh increases in P, which are thought to increase N yield by decreasing residence times within the landscape. For some parts of the study area, however, we found that projected P and T conditions may result in increasing N yields. In some watersheds on the coast of the Pacific Northwest and Northern California, for example, where projected increases in T are more moderate compared to projected increases in P, climatic conditions will favor increases in N yield. For these regions, our analysis suggests that projected changes in P and T, holding all other variables constant, would result in N yield increases of up to 15% in 2050 and 25% in 2090. Nitrogen pollution in these waterbodies, however, is less of a current concern compared to waterbodies like the Chesapeake Bay and Gulf of Mexico.

This work contributes to a growing body of literature that explores the impact of climate change on N yield. The results of one of the first studies examining this for watersheds in the Chesapeake Bay predicted increases in N yield with projected P changes, but did not consider the impacts due to projected changes in T (Howarth *et al.*, 2006). Recent studies using the SWAT model and GCM projections of P and T conducted for the Upper Mississippi River Basin show the uncertainty in projected N yield changes (Jha, *et al.*, 2015; Panagopoulos *et al.*, 2014). Our results, however, agree with those of Panagopoulos *et al.* (2014) and indicate that N yield to these waterbodies may decrease on average as a result of projected changes in P and T.

Climate change will only be a part of the larger picture for determining future N yield and, ultimately, N concentrations in waterbodies. Many other factors will be at play including N inputs to watersheds, land use and cover changes, and the role of best management practices for N removal. Despite this complexity, the results of this study suggest that water managers, especially in regions identified in this study where future climatic conditions may increase N yield, take projected P and T long term trends into consideration when developing more detailed and localized models and plans for mitigating N pollution for impaired waterbodies.

ACKNOWLEDGMENTS

This work was supported by the National Science Foundation under the grant CBET-0846244. The authors acknowledge the Universities of South Carolina and Washington where the coauthors were previously employed when this research was initiated. The authors also wish to thank Richard Alexander from the USGS and the editor and reviewers of the manuscript for their constructive comments and suggestions for improving the manuscript.

LITERATURE CITED

Alam, M.J. and J.L. Goodall, 2012. Toward Disentangling the Effect of Hydrologic and Nitrogen Source Changes from 1992 to 2001 on Incremental Nitrogen Yield in the Contiguous United States. Water Resources Research 48. DOI:10.1029/2011WR010967.

Alexander, R.B., P.J. Johnes, E.W. Boyer, and R.A. Smith, 2002. A Comparison of Models for Estimating the Riverine Export of Nitrogen from Large Watersheds. Biogeochemistry 57:295–339. DOI: 10.1023/A:1015752801818.

Alexander, R.B., R.A. Smith, and G.E. Schwarz, 2000. Effect of Stream Channel Size on the Delivery of Nitrogen to the Gulf of Mexico. Nature 403:758–761. DOI: 10.1038/35001562.

Alexander, R.B., R.A. Smith, G.E. Schwarz, E.W. Boyer, J. V. Nolan, and J.W. Brakebill, 2008. Differences in Phosphorus and Nitrogen Delivery to The Gulf of Mexico from the Mississippi River Basin. Environmental Science & Technology 42:822–830. DOI: 10.1021/es0716103.

Baker, N. and H. Huang, 2014. A Comparative Study of Precipitation and Evaporation between CMIP3 and CMIP5 Climate Model Ensembles in Semiarid Regions. J. Climate 27:3731–3749. DOI:10.1175/JCLI-D-13-00398.1.

Blois, J.L., J.W. Williams, M.C. Fitzpatrick, S.T. Jackson, and S. Ferrier, 2013. Space Can Substitute for Time in Predicting Climate-Change Effects on Biodiversity. Proceedings of the National Academy of Sciences 110:9374–9379. DOI: 10.1073/pnas.1220228110.

Brekke, L.D., M.D. Dettinger, E.P. Maurer, and M. Anderson, 2008. Significance of Model Credibility in Estimating Climate Projection Distributions for Regional Hydroclimatological Risk Assessments. Climatic Change 89:371–394. DOI: 10.1007/s10584-007-9388-3.

Brown, J.B., L.A. Sprague, and J.A. Dupree, 2011. Nutrient Sources and Transport in the Missouri River Basin, with Emphasis on the Effects of Irrigation and Reservoirs: Nutrient Sources and Transport in the Missouri River Basin, With Emphasis on the Effects of Irrigation and Reservoirs. JAWRA Journal of the American Water Resources Association 47:1034–1060. DOI: 10.1111/j.1752-1688.2011.00584.x.

Collins, W.D., C.M. Bitz, M.L. Blackmon, G.B. Bonan, C.S. Bretherton, J.A. Carton, P. Chang, S.C. Doney, J.J. Hack, T.B. Henderson, J.T. Kiehl, W.G. Large, D.S. McKenna, B.D. Santer, and R.D. Smith, 2006. The Community Climate System Model Version 3 (CCSM3). Journal of Climate 19:2122–2143. DOI: 10.1175/JCLI3761.1.

Caroline A. Davis, A.S. Ward, A.J. Burgin, T.D. Loecke, D.A. Riveros-Iregui, D.J. Schnoebelen, C.L. Just, S.A. Thomas, L.J. Weber, and M.A. St. Clair, 2014. Antecedent Moisture Controls on Stream Nitrate Flux in an Agricultural Watershed. Journal of Environmental Quality 43:1494-1503. DOI: 10.2134/jeq2013.11.0438.

Deacon, J.R., C.J. Lee, P.L. Toccalino, M.P. Warren, N.T. Baker, C.G. Crawford, R.G. Gilliom, and M.D. Woodside, 2015. Tracking Water-Quality of the Nation’s Rivers and Streams. U.S. Geological Survey Web page, <http://cida.usgs.gov/quality/rivers>. DOI:10.5066/F70G3H51.

Delworth, T.L., A.J. Broccoli, A. Rosati, R.J. Stouffer, V. Balaji, J.A. Beesley, W.F.

Cooke, K.W. Dixon, J. Dunne, K.A. Dunne, J.W. Durachta, K.L. Findell, P. Ginoux, A. Gnanadesikan, C.T. Gordon, S.M. Griffies, R. Gudgel, M.J. Harrison, I.M. Held, R.S. Hemler, L.W. Horowitz, S.A. Klein, T.R. Knutson, P.J. Kushner, A.R. Langenhorst, H.-C. Lee, S.-J. Lin, J. Lu, S.L. Malyshev, P.C.D. Milly, V. Ramaswamy, J. Russell, M.D. Schwarzkopf, E. Shevliakova, J.J. Sirutis, M.J. Spelman, W.F. Stern, M. Winton, A.T. Wittenberg, B. Wyman, F. Zeng, and R. Zhang, 2006. GFDL's CM2 Global Coupled Climate Models. Part I: Formulation and Simulation Characteristics. Journal of Climate 19:643–674. DOI: 10.1175/JCLI3629.1.

Diansky, N. and E. Volodin, 2002. Simulation of Present-Day Climate with a Coupled Atmosphere-Ocean General Circulation Model. Izvestiya Atmospheric and Oceanic Physics 38:732–747.

Diaz, R.J., 2001. Overview of Hypoxia around the World. Journal of Environmental Quality 30:275.

Diaz, R.J., and R. Rosenberg, 2008. Spreading Dead Zones and Consequences for Marine Ecosystems. Science 321:926–929. DOI: 10.1126/science.1156401.

Donner, S.D., Christopher J. Kucharik, and Michael Oppenheimer, 2004. The Influence of Climate on in-Stream Removal of Nitrogen. Geophysical Research Letters 31. DOI:10.1029/2004GL020477.

Donner, S.D. and C.J. Kucharik, 2003. Evaluating the Impacts of Land Management and Climate Variability on Crop Production and Nitrate Export across the Upper Mississippi Basin. Global Biogeochemical Cycles 17. DOI:10.1029/2001GB001808.

Drewry, J.J., L.T.H. Newham, and R.S.B. Greene, 2011. Index Models to Evaluate the Risk of Phosphorus and Nitrogen Loss at Catchment Scales. Journal of Environmental Management 92:639–649. DOI: 10.1016/j.jenvman.2010.10.001.

Environmental Protection Agency (U.S.), 2001. National Coastal Condition Report EPA-620/R-01/005. Office of Research and Development/Office of Water, Washington, D.C.

Flato, G.M. and G.J. Boer, 2001. Warming Asymmetry in Climate Change Simulations. Geophysical Research Letters 28:195–198. DOI: 10.1029/2000GL012121.

Furevik, T., M. Bentsen, H. Drange, I.K.T. Kindem, N.G. Kvamst, and A. Sorteberg, 2003. Description and Evaluation of the Bergen Climate Model: ARPEGE Coupled with MICOM. Climate Dynamics 21:27–51. DOI: 10.1007/s00382-003-0317-5.

Goolsby, D.A., W.A. Battaglin, G.B. Lawrence, R.S. Artz, B.T. Aulenbach, R.P. Hooper, D.R. Keeney, and G.J. Stensland, 1999. Flux and Sources of Nutrients in the Mississippi–Atchafalaya River Basin. NOAA Coastal Ocean Program, Decision Analysis Series No. 17. National Oceanic and Atmospheric Administration, National Ocean Service, Coastal Ocean Program.

Grizzetti, B., F. Bouraoui, and G. De Marsily, 2005. Modelling Nitrogen Pressure in River Basins: A Comparison between a Statistical Approach and the Physically-Based SWAT Model. Physics and Chemistry of the Earth, Parts A/B/C 30:508–517. DOI: 10.1016/j.pce.2005.07.005.

Gruber, N. and J. Galloway, 2008. An Earth-System Perspective of the Global Nitrogen Cycle. Nature 451:293-296. DOI:10.1038/nature06592.

Hall R. O. Jr., Tank, J. L. Tank, Sobota D. J. Sobota, P. J. Mulholland, J. M. O'Brien, W. K. Dodds, J. R. Webster, H. M. Valett, B. J. Peterson, J. L. Meyer, W. H.

McDowell, S. L. Johnson, S. K. Hamilton, N. B. Grimm, S. V. Gregory, C. N. Dahm, L. W. Cooper, L. R. Ashkenas, S. M. Thomas, R. W. Sheibley, J. D. Potter, B. R. Niederlehner, L. T. Johnson, A. M. Helton, C. M. Crenshaw, A. J. Burgin, M. J. Bernot, J. J. Beaulieu, C. P. Arangob, 2009. Nitrate Removal in Stream Ecosystems Measured by 15N Addition Experiments: Total Uptake. Limnology and Oceanography 54, DOI: 10.4319/lo.2009.54.3.0653.

Han, H., J.D. Allan, and D. Scavia, 2009. Influence of Climate and Human Activities on the Relationship between Watershed Nitrogen Input and River Export. Environmental Science & Technology 43:1916–1922. DOI: 10.1021/es801985x.

Hasumi, H. and S. Emori, 2004. K-1 Coupled Model (MIROC) Description. K-1 Technical Report, 1. Center for Climate System Research, University of Tokyo. Tokyo.

Hong, B., D. P. Swaney, and R. W. Howarth, 2013. Estimating Net Anthropogenic Nitrogen Inputs to US Watersheds: Comparison of Methodologies. Environmental Science & Technology 47.10: 5199-5207. DOI: 10.1021/es303437c.

Hoos, A.B. and G. McMahon, 2009. Spatial Analysis of Instream Nitrogen Loads and Factors Controlling Nitrogen Delivery to Streams in the Southeastern United States Using Spatially Referenced Regression on Watershed Attributes (SPARROW) and Regional Classification Frameworks. Hydrological Processes 23:2275–2294. DOI: 10.1002/hyp.7323.

Howarth, R., D. Swaney, G. Billen, J. Garnier, B. Hong, C. Humborg, P. Johnes, C.-M. Mörth, and R. Marino, 2012. Nitrogen Fluxes from the Landscape Are Controlled by Net Anthropogenic Nitrogen Inputs and by Climate. Frontiers in Ecology and the Environment 10:37–43. DOI: 10.1890/100178.

Howarth, R., F. Chan, D.J. Conley, J. Garnier, S.C. Doney, R. Marino, G. Billen, 2011. Coupled Biogeochemical Cycles: Eutrophication and Hypoxia in Temperate Estuaries and Coastal Marine Ecosystems. Frontiers in Ecology and the Enironment 9:18-26. DOI: 10.1890/100008.

Howarth, R.W., D.P. Swaney, E.W. Boyer, R. Marino, N. Jaworski, and C. Goodale, 2006. The Influence of Climate on Average Nitrogen Export from Large Watersheds in the Northeastern United States. Biogeochemistry 79:163–186. DOI: 10.1007/s10533-006-9010-1.

Howden, N.J.K., T.P. Burt, F. Worrall, and M.J. Whelan, 2011. Monitoring Fluvial Water Chemistry for Trend Detection: Hydrological Variability Masks Trends in Datasets Covering Fewer than 12 Years. Journal of Environmental Monitoring 13:514. DOI: 10.1039/c0em00722f.

Jha, M., P. Gassman, and Y. Panagopoulos, 2015. Regional Changes in Nitrate Loadings in the Upper Mississippi River Basin Under Predicted Mid-century Climate. Regional Environmental Change 15:449-460. DOI: 10.1007/s10113-013-0539-y.

Jha, M.K., P.W. Gassman, S. Secchi, and J.G. Arnold, 2006. Upper Mississippi River Basin modeling system part 2: baseline simulation results. In: Singh V.P., Xu Y.J. (eds) Coastal Hydrology and Processes. Water Resources Publications, Highland Ranch, CO, ISBN: 1-887201-46-7.

Jungclaus, J.H., N. Keenlyside, M. Botzet, H. Haak, J.-J. Luo, M. Latif, J. Marotzke, U. Mikolajewicz, and E. Roeckner, 2006. Ocean Circulation and Tropical Variability in the Coupled Model ECHAM5/MPI-OM. Journal of Climate 19:3952–3972. DOI:

10.1175/JCLI3827.1.
Kaushal, S.S., P.M. Groffman, L.E. Band, C.A. Shields, R.P. Morgan, M.A. Palmer, K.T. Belt, C.M. Swan, S.E.G. Findlay, and G.T. Fisher, 2008. Interaction between Urbanization and Climate Variability Amplifies Watershed Nitrate Export in Maryland. Environmental Science & Technology 42:5872–5878. DOI: 10.1021/es800264f.
Kemp, W.M., W. R. Boynton, J. E. Adolf, D. F. Boesch, W. C. Boicourt, G. Brush, J. C. Cornwell, T. R. Fisher, P. M. Glibert, J. D. Hagy, L. W. Harding, E. D. Houde, D. G. Kimmel, W. D. Miller, R. I. E. Newell, M. R. Roman, E. M. Smith, J. C. Stevenson, 2005. Eutrophication of Chesapeake Bay: Historical Trends and Ecological Interactions. Marine Ecology Progress Series 303:1-29. DOI: 10.3354/meps303001.
Legutke, S. and R. Ross, 1999. The Hamburg Atmosphere-Ocean Coupled Circulation Model ECHO-G. Technical Report. German Climate Computer Centre (DKRZ). Hamburg, Germany.
Lim, K.J., B.A. Engel, Z. Tang, S. Muthukrishnan, J. Choi, and K. Kim, 2006. Effects of Calibration on L-THIA GIS Runoff and Pollutant Estimation. Journal of Environmental Management 78:35–43. DOI: 10.1016/j.jenvman.2005.03.014.
Marti, O., P. Braconnot, J. Bellier, R. Benshila, S. Bony, P. Brockmann, P. Cadule, A. Caubel, S. Denvil, J.-L. Dufresne, L. Fairhead, M.-A. Filiberti, M.-A. Foujols, T.T. Fichefet, P. Friedlingstein, H. Gosse, J.-Y. Grandpeix, F.F. Hourdin, G. Krinner, C. Lévy, G. Madec, I. Musat, N. de Noblet, J. Polcher, and C. Talandier, 2006. The New IPSL Climate System Model: IPSL-CM4. Institut Pierre-Simon Laplace (IPSL).
Maurer, E.P., L. Brekke, T. Pruitt, and P.B. Duffy, 2007. Fine-Resolution Climate Projections Enhance Regional Climate Change Impact Studies. Eos, Transactions American Geophysical Union 88:504–504.
McIsaac, G.F., M.B. David, and G.Z. Gertner, 2016. Illinois River Nitrate-Nitrogen Concentrations and Loads: Long-term Variation and Association with Watershed Nitrogen Inputs. Journal of Environmental Quality 45:1268–1275. DOI:10.2134/jeq2015.10.0531.
Meehl, G.A., C. Covey, K.E. Taylor, T. Delworth, R.J. Stouffer, M. Latif, B. McAvaney, and J.F.B. Mitchell, 2007. THE WCRP CMIP3 Multimodel Dataset: A New Era in Climate Change Research. Bulletin of the American Meteorological Society 88:1383–1394. DOI: 10.1175/BAMS-88-9-1383.
Moore, R.B., C.M. Johnston, R.A. Smith, and B. Milstead, 2011. Source and Delivery of Nutrients to Receiving Waters in the Northeastern and Mid-Atlantic Regions of the United States1: Source and Delivery of Nutrients to Receiving Waters in the Northeastern and Mid-Atlantic Regions of the United States. JAWRA Journal of the American Water Resources Association 47:965–990.
Mulholland P. J., R. O. Hall, D. J. Sobota, W. K. Dodds, E. G. Findlay Stuart, N. B. Grimm, S. K. Hamilton, W. H. McDowell, J. M. O'Brien, J. L. Tank, L. R. Ashkenas, L. W. Cooper, C. N. Dahm, S. V. Gregory, S. L. Johnson, J. L. Meyer, B. J. Peterson, G. C. Poole, H. M. Valett, J. R. Webster, C. P. Arango, J. J. Beaulieu, M. J. Bernot, A. J. Burgin, C. L. Crenshaw, A. M. Helton, L. T. Johnson, B. R. Niederlehner, J. D. Potter, R. W. Sheibley, S. M. Thomasn, 2009. Nitrate Removal

in Stream Ecosystems Measured by 15N Addition Experiments: Denitrification. Limnology and Oceanography 54. DOI: 10.4319/lo.2009.54.3.0666.

Najjar, R.G., C.R. Pyke, M.B. Adams, D. Breitburg, C. Hershner, M. Kemp, R. Howarth, M.R. Mulholland, M. Paolisso, D. Secor, K. Sellner, D. Wardrop, and R. Wood, 2010. Potential Climate-Change Impacts on the Chesapeake Bay. Estuarine, Coastal and Shelf Science 86:1–20. DOI: 10.1016/j.ecss.2009.09.026.

Nangia, V., D.J. Mulla, P.H. Gowda, 2010. Precipitation Changes Impact Stream Discharge, Nitrate-Nitrogen Load More Than Agricultural Management Changes. Journal of Environmental Quality 39:2063-2071. DOI: 10.2134/jeq2010.0105.

National Atmospheric Deposition Program (NADP), 2010. National Atmospheric Deposition Program (NRSP-3). Natl. Atmos. Depos. Prog. Prog. Off., Ill. State Water Surv., Champaign.

National Research Council (U.S.), 2000. Clean Coastal Waters: Understanding and Reducing the Effects of Nutrient Pollution. National Academy Press, Washington, D.C.

Nolan, J. V., J. W.Brakebill, R.B. Alexander, and G.E. Schwarz, 2002. Enhanced River Reach File 2. U.S. Geological Survey Open-File Report 02-40. Reston, Virginia.

Panagopoulos, Y. P.W. Gassman, R. W. Arritt, D.E. Herzmann, T.D. Campbell, M. K. Jha, C. L. Kling, R. Srinivasan, M. White, J. G. Arnold, 2014. Surface water quality and cropping systems sustainability under a changing climate in the Upper Mississippi River Basin. Journal of Soil and Water Conservation 69:483-494. DOI: 10.2489/jswc.69.6.483.

Paul, M.J. and J.L. Meyer, 2001. Streams in the Urban Landscape. Annual Review of Ecology and Systematics 32:333–365.Pickett, S.T.A., 1989. Space-for-Time Substitution as an Alternative to Long-Term Studies. Long-Term Studies in Ecology. Springer New York, New York, NY, pp. 110–135.

Pierce, D.W., T.P. Barnett, B.D. Santer, and P.J. Gleckler, 2009. Selecting Global Climate Models for Regional Climate Change Studies. Proceedings of the National Academy of Sciences 106:8441–8446.

Qian, S.S., K.H. Reckhow, J. Zhai, and G. McMahon, 2005. Nonlinear Regression Modeling of Nutrient Loads in Streams: A Bayesian Approach. Water Resources Research 41. DOI:10.1029/2005WR003986. DOI: 10.1029/2005WR003986.Rebich, R.A., N.A. Houston, S. V. Mize, D.K. Pearson, P.B. Ging, and C. Evan Hornig, 2011. Sources and Delivery of Nutrients to the Northwestern Gulf of Mexico from Streams in the South-Central United States1: Sources and Delivery of Nutrients to the Northwestern Gulf of Mexico From Streams in the South-Central United States. JAWRA Journal of the American Water Resources Association 47:1061–1086.

Reichler, T. and J. Kim, 2008. How Well Do Coupled Models Simulate Today’s Climate? Bulletin of the American Meteorological Society 89:303–311.

Robertson, D.M. and D.A. Saad, 2011. Nutrient Inputs to the Laurentian Great Lakes by Source and Watershed Estimated Using SPARROW Watershed Models: Nutrient Inputs to the Laurentian Great Lakes by Source and Watershed Estimated Using SPARROW Watershed Models. JAWRA Journal of the American Water Resources Association 47:1011–1033. DOI: 10.1111/j.1752-1688.2011.00574.x.

Ruddy, B., Lorenz, D., and Mueller, D., 2006. County-Level Estimates of Nutrient Inputs to the Land Surface of the Conterminous United States. U.S. Geological Survey

Open-File Report 1982-2001. Reston, Virginia.

Russell, G.L., J.R. Miller, D. Rind, R.A. Ruedy, G.A. Schmidt, and S. Sheth, 2000. Comparison of Model and Observed Regional Temperature Changes during the Past 40 Years. Journal of Geophysical Research 105:14891. DOI: 10.1029/2000JD900156.

Salas-Mélia, D., F. Chauvin, M. Déqué, H. Douville, J.F. Gueremy, P. Marquet, S. Planton, J.F. Royer, and S. Tyteca, 2005. Description and Validation of the CNRM-CM3 Global Coupled Model. CNRM Working Note 103.

Schaefer, S.C. and M. Alber, 2007. Temperature Controls a Latitudinal Gradient in the Proportion of Watershed Nitrogen Exported to Coastal Ecosystems. Biogeochemistry 85:333–346. DOI: 10.1007/s10533-007-9144-9.

Schwarz, G.E., A.B. Hoos, R.B. Alexander, and R.A. Smith, 2006. The SPARROW Surface Water-Quality Model: Theory, Application and User Documentation. U.S. Geological Survey Techniques and Methods. Section B, Book 6. U.S. Geological Survey, Reston, Virginia.

Seaber, P.R., F.P. Kapinos, and G.L. Knapp, 1987. Hydrologic Unit Maps. United States Geological Survey Water-Supply Paper 2294.

Seitzinger, S.P., 1988. Denitrification in Freshwater and Coastal Marine Ecosystems: Ecological and Geochemical Significance. Limnology and Oceanography 33:702–724.

Singa, E. and A. Michalak, 2016. Precipitation Dominates Interannual Variability of Riverine Nitrogen Loading across the Continental United States. Environmental Science and Technology 50:12874-12884. DOI: 10.1021/acs.est.6b04455.

Smith, R.A., G.E. Schwarz, and R.B. Alexander, 1997. Regional Interpretation of Water-Quality Monitoring Data. Water Resources Research 33:2781–2798.

Smith, R.A., G.E. Schwarz, J.W. Brakebill, A.B. Hoos, R.B. Moore, J. Shih, A.W. Nolin, M. Macauley, and R.B. Alexander, 2013. Seasonally-Dynamic SPARROW Modeling of Nitrogen Flux Using Earth Observation Data. AGU Fall Meeting Abstracts:G383.

Sobota, D.J., J.A. Harrison, and R.A. Dahlgren, 2009. Influences of Climate, Hydrology, and Land Use on Input and Export of Nitrogen in California Watersheds. Biogeochemistry 94: 43. DOI:10.1007/s10533-009-9307-y.

Sun, L., K.E. Kunkel, L.E. Stevens, A. Buddenberg, J.G. Dobson, and D.R. Easterling, 2015. Regional Surface Climate Conditions in CMIP3 and CMIP5 for the United States: Differences, Similarities, and Implications for the U.S. National Climate Assessment. NOAA Technical Report NESDIS 114. DOI:10.7289/V5RB72KG.

U.S. Geological Survey, 2004. HYDRO1k Elevation Derivative Database. Earth Resources Observation and Science (EROS) Center, Sioux Falls, South Dakota.

Van Meter, K.J., N.B. Basu, J.J. Veenstra, and C.L. Burras, 2016. The Nitrogen Legacy: Emerging Evidence of Nitrogen Accumulation in Anthropogenic Landscapes. Environmental Research Letters 11 035014. DOI:10.1088/1748-9326/11/3/035014.

Veraart, A.J., J.J.M. de Klein, and M. Scheffer, 2011. Warming Can Boost Denitrification Disproportionately Due to Altered Oxygen Dynamics L. Stal (Editor). PLoS ONE 6:e18508. DOI: 10.1371/journal.pone.0018508.

Vitousek, P.M., J.D. Aber, R.W. Howarth, G.E. Likens, P.A. Matson, D.W. Schindler, W.H. Schlesinger, and D.G. Tilman, 1997. Human Alteration of the Global Nitrogen

Cycle: Sources and Consequences. Ecological Applications 7:737–750. DOI: 10.2307/2269431.
Wan, R., S. Cai, H. Li, G. Yang, Z. Li, and X. Nie, 2014. Inferring Land Use and Land Cover Impact on Stream Water Quality Using a Bayesian Hierarchical Modeling Approach in the Xitiaoxi River Watershed, China. Journal of Environmental Management 133:1–11. DOI: 10.1016/j.jenvman.2013.11.035.
Wise, D.R. and H.M. Johnson, 2011. Surface-Water Nutrient Conditions and Sources in the United States Pacific Northwest: Surface-Water Nutrient Conditions and Sources in the United States Pacific Northwest. JAWRA Journal of the American Water Resources Association 47:1110–1135. DOI: 10.1111/j.1752-1688.2011.00580.x.
Ye, L. and N.B. Grimm, 2013. Modelling Potential Impacts of Climate Change on Water and Nitrate Export from a Mid-Sized, Semiarid Watershed in the US Southwest. Climatic Change 120:419–431. DOI: 10.1007/s10584-013-0827-z.
Yukimoto, S., A. Noda, A. Kitoh, M. Sugi, Y. Kitamura, M. Hosaka, K. Shibata, S. Maeda, and T. Uchiyama, 2001. The New Meteorological Research Institute Coupled GCM(MRI-CGCM2). Model Climate and Variability. Papers in Meteorology and Geophysics 51:47–88.
Zaehle, S. and A.D. Friend, 2010. Carbon and Nitrogen Cycle Dynamics in the O-CN Land Surface Model: 1. Model Description, Site-Scale Evaluation, and Sensitivity to Parameter Estimates. Global Biogeochemical Cycles 24. DOI:10.1029/2009GB003521.

Table 1. The 14 General Climate Models (GCMs) used for P and T projections.

Climate Models	Institutions, sponsoring agency, country	References
BCCR-BCM 2.0	Bjerknes Center for Climate Research	(Furevik *et al.*, 2003)
CGCM3.1 (T47)	Canadian Centre for Climate Modeling & Analysis	(Flato and Boer, 2001)
CNRM-CM3	Météo-France / Centre National de Recherches Météorologiques, France	(Salas-Mélia *et al.*, 2005)
GFDL-CM2.0	US Dept. of Commerce / NOAA / Geophysical Fluid Dynamics Laboratory, USA	(Delworth *et al.*, 2006)
GFDL-CM2.1	US Dept. of Commerce / NOAA / Geophysical Fluid Dynamics Laboratory, USA	(Delworth *et al.*, 2006)
GISS-ER	NASA / Goddard Institute for Space Studies, USA	(Russell *et al.*, 2000)
INM-CM3.0	Institute for Numerical Mathematics, Russia	(Diansky and Volodin, 2002)
IPSL-CM4	Institut Pierre Simon Laplace, France	(Marti *et al.*, 2006)
MIROC3.2 (medres)	Center for Climate System Research (The University of Tokyo), National Institute for Environmental Studies, an Frontier Research Center for Global Change (JAMSTEC), Japan	(Hasumi and Emori, 2004)
ECHO-G	Meteorological Institute of the University of Bonn, Meteorological Research Institute of KMA	(Legutke and Ross, 1999)
ECHAM5/MPI-OM	Max Planck Institute for Meteorology, Germany	(Jungclaus *et al.*, 2006)
MRI-CGCM2.3.2	Meteorological Research Institute, Japan	(Yukimoto *et al.*, 2001)
CCSM3	National Center for Atmospheric Research, USA	(Collins *et al.*, 2006)
UKMO-HadCM3	Hadley Centre for Climate Prediction and Research / Met Office, UK	(Collins *et al.*, 2006)

Table 2. Calibration results for the A2 and B1 scenarios of the base year (1992) SPARROW model. Provided numbers are the low and high calibration results across the 14 GCM output data sets.

Nonlinear Least Squares Calibration		**A2 Scenarios**			**B1 Scenarios**		
Model Parameters	Coefficient Units	Coefficient (Mean)	Standard Error	p-Value	Coefficient (Mean)	Standard Error	p-Value
Nitrogen Source Variables, β							
Population Related Sources	kg $person^{-1}$ yr^{-1}	3.132~3.354	0.746~0.785	<0.05	3.126~3.339	0.751~0.785	<0.05
Atmospheric Deposition	dimensionless	0.562~0.680	0.146~0.153	<0.05	0.560~0.670	0.146~0.153	<0.05
Fertilizer Application	dimensionless	0.217~0.230	0.044~0.046	<0.05	0.217~0.230	0.044~0.046	<0.05
Livestock Waste Production	dimensionless	0.041~0.051	0.059~0.063	0.401~0.501	0.041~0.051	0.060~0.063	0.402~0.495
Non Agricultural Land	kg km^{-1} yr^{-1}	194.8~232.0	41.98~45.47	<0.05	199.0~232.0	42.27~45.48	<0.05
Land-Water Delivery Variables, α'							
Soil Permeability	in hr^{-1}	-0.089~-0.079	0.017~0.017	<0.05	-0.090~-0.080	0.017~0.017	<0.05
Drainage Density	km^{-1}	0.913~1.158	0.785~0.807	0.143~0.258	0.870~1.155	0.783~0.812	0.144~0.285
Mean Annual Air Temp. (T)	$^{\circ}C$	-0.064~-0.057	0.008~0.008	<0.05	-0.063~-0.058	0.008~0.008	<0.05
Precipitation (P)	10^2 mm	0.009~0.010	0.001~0.001	<0.05	0.009~0.010	0.001~0.001	<0.05
Instream Losses, κ'							
κ_1 ($Q \leq 28.3\ m^3/s$)	day^{-1}	0.216~0.229	0.028~0.029	<0.05	0.215~0.229	0.028~0.029	<0.05
κ_2 ($28.3\ m^3/s < Q < 283\ m^3/s$)	day^{-1}	0.216~0.229	0.023~0.024	<0.05	0.047~0.052	0.023~0.024	<0.05
Reservoir Attenuation, κ_r	m yr^{-1}	6.885~7.112	1.834~1.890	<0.05	6.896~7.114	1.836~1.890	<0.05

Table 3. Names of the hydrologic regions (2-digit HUC) for the contiguous United States (Seaber *et al.*, 1987). A map of the basins is provided in Figure 8.

Region No	Region Name	Region No	Region Name
Region 01	New England	Region 10	Missouri
Region 02	Mid-Atlantic	Region 11	Arkansas-White-Red
Region 03	South Atlantic-Gulf	Region 12	Texas-Gulf
Region 04	Great Lakes	Region 13	Rio Grande
Region 05	Ohio	Region 14	Upper Colorado
Region 06	Tennessee	Region 15	Lower Colorado
Region 07	Upper Mississippi	Region 16	Great Basin
Region 08	Lower Mississippi	Region 17	Pacific Northwest
Region 09	Souris-Red-Rainy	Region 18	California

Figure 1. T (º C) predictions over different time periods for the contiguous United States for the A2 and B1 emission scenarios. Here 1992, 2030, 2050 and 2090 refer to the ensemble average of 20 years T data around each year (e.g., 2030 refers to the ensemble average of 2020-2039) from the 14 GCMs used in this study.

Figure 2. P (mm) predictions over different time periods for the contiguous United States for the A2 and B1 emission scenarios. Here 1992, 2030, 2050 and 2090 refer to the ensemble average of 20 years P data around each year (e.g., 2030 refers to the ensemble average of 2020-2039) from the 14 GCMs used in this study.

Figure 3. Spatial patterns in total N yield (kg/ha yr) for baseline conditions. The estimates were produced using the SPARROW model and GCM output averaged across an ensemble of 14 models for the A2 (high) and B1 (low) emission scenarios.

Figure 4. Evaluation of 1992 calibrated model performance for predicted log of flux versus actual log of flux of TN. The r^2 and RMSE values compare model performance with observed water quality conditions from the 354 available monitoring stations.

Figure 5. Evaluation of calibrated model applied to 2001 dataset. The r^2 value compares model performance with observed water quality conditions from the 122 available monitoring stations.

Figure 6. Incremental N yield change (%) predictions for different time periods under the A2 and B1 emission scenarios over the contiguous United States. This is the average of the SPARROW model outputs from each of the 14 different GCM predictions for future P and T conditions.

Figure 7. Regional changes in incremental N yield (kg/ha yr) over different time periods from 14 GCMs with A2 (high) and B1 (low) emission scenarios. The regions consist of major river basins and are represented by a 2-digit Hydrologic Unit Code (HUC).

Figure 8. Hydrologic Unit Code (HUC) for the 2-digit HUC boundaries in the contiguous United States (USGS, 2013). These regions contain the drainage area of a major river or a series of rivers. The average area of these regions is 177,560 mi^2. The SPARROW model output was summarized and presented at this regional level to compare the model outputs at the major river basin scale.

Figure 9. N yield change (%) for given changes in T (ºC) and P (mm) within each level-8 watershed using the 14 GCMs and the A2 (high) or B1 (low) emission scenarios.

Figure 1.

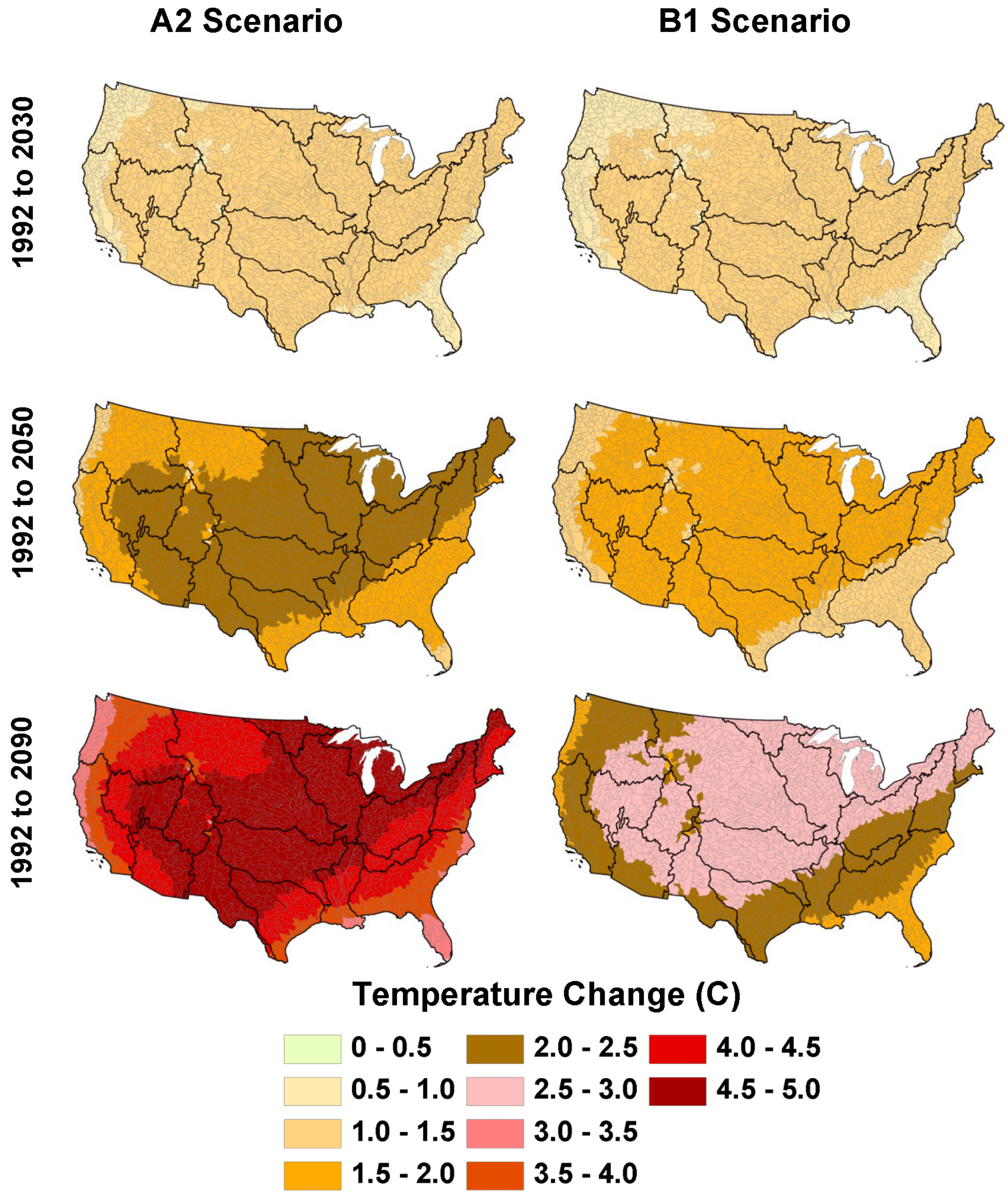
A2 Scenario
B1 Scenario
1992 to 2030
1992 to 2050
1992 to 2090
Temperature Change (C)
0 - 0.5
0.5 - 1.0
1.0 - 1.5
1.5 - 2.0
2.0 - 2.5
2.5 - 3.0
3.0 - 3.5
3.5 - 4.0
4.0 - 4.5
4.5 - 5.0

Figure 2.

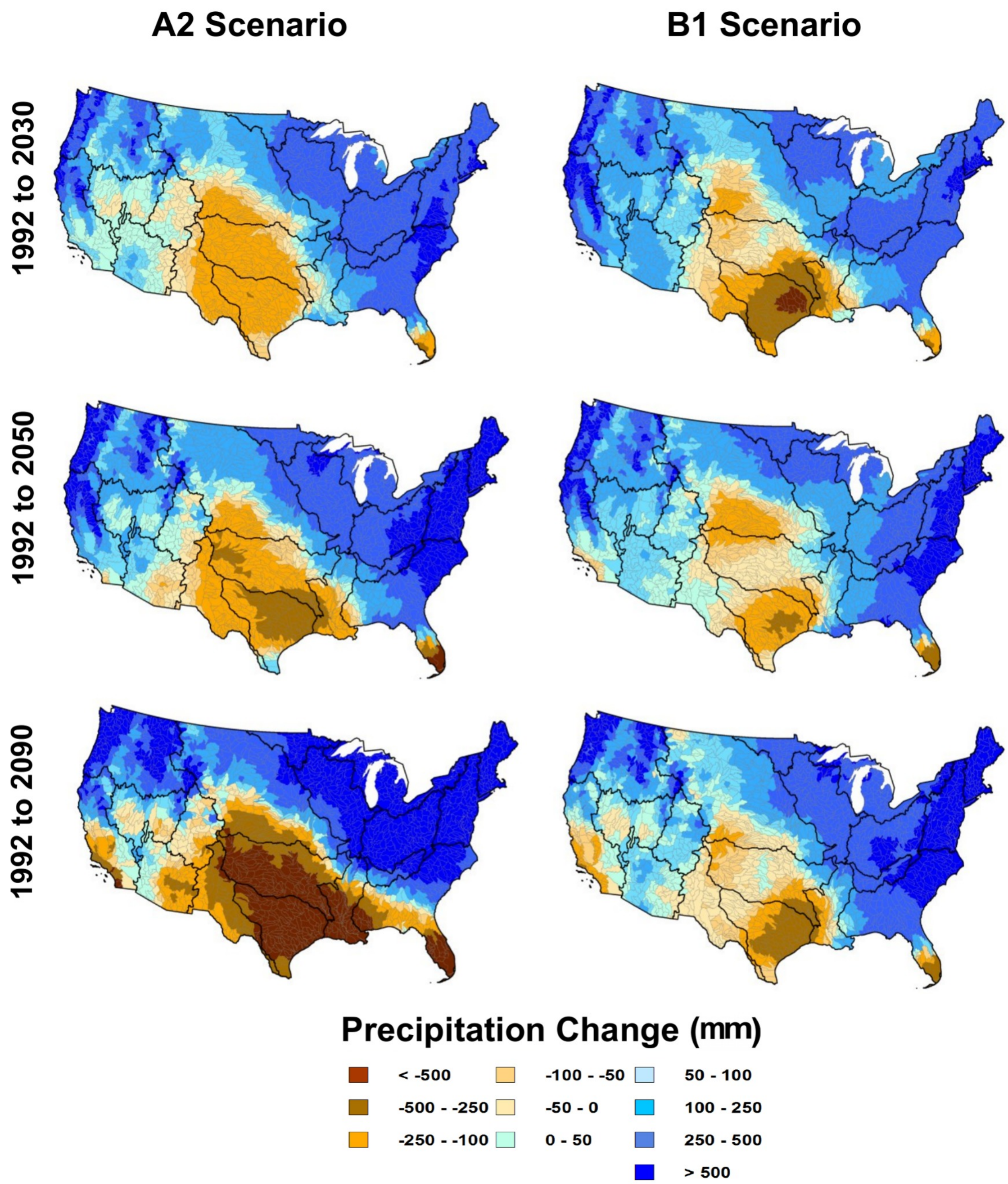
A2 Scenario
B1 Scenario
1992 to 2030
1992 to 2050
1992 to 2090
Precipitation Change (mm)
< -500
-500 - -250
-250 - -100
-100 - -50
-50 - 0
0 - 50
50 - 100
100 - 250
250 - 500
> 500

Figure 3.

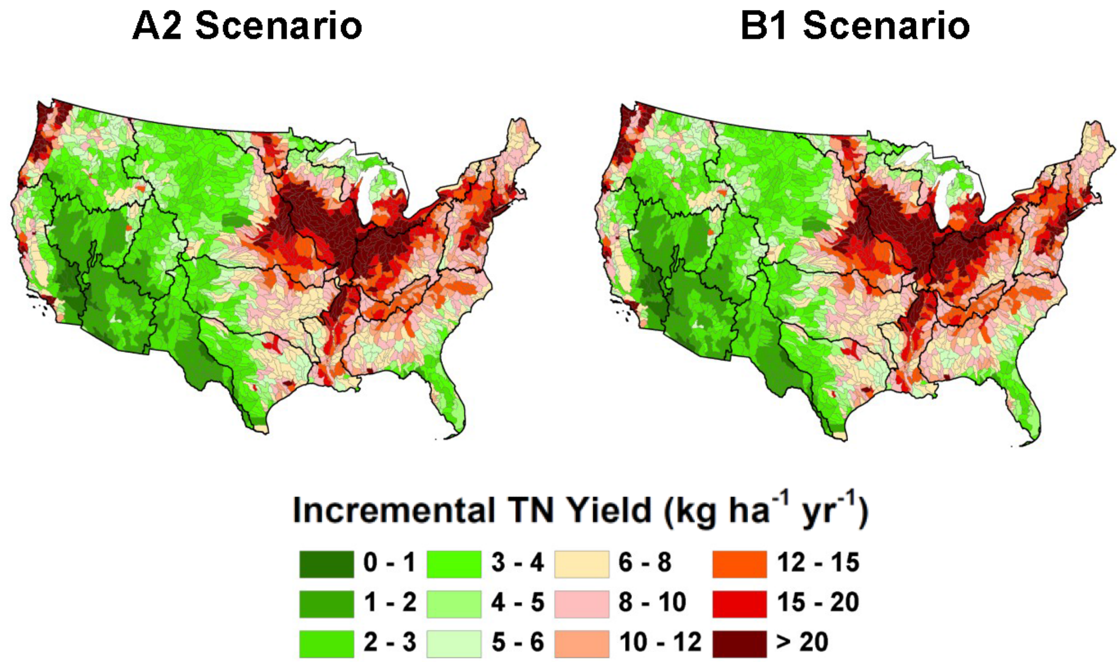
A2 Scenario
B1 Scenario
Incremental TN Yield (kg ha^{-1} yr^{-1})
0 - 1
1 - 2
2 - 3
3 - 4
4 - 5
5 - 6
6 - 8
8 - 10
10 - 12
12 - 15
15 - 20
> 20

Figure 4.

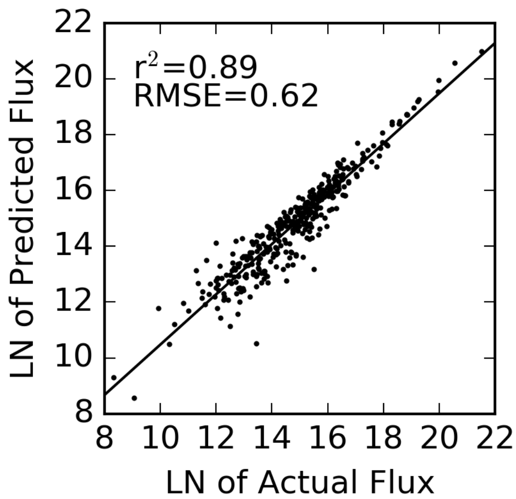
r²=0.89
RMSE=0.62
LN of Predicted Flux
LN of Actual Flux
8 10 12 14 16 18 20 22
8 10 12 14 16 18 20 22

Figure 5.

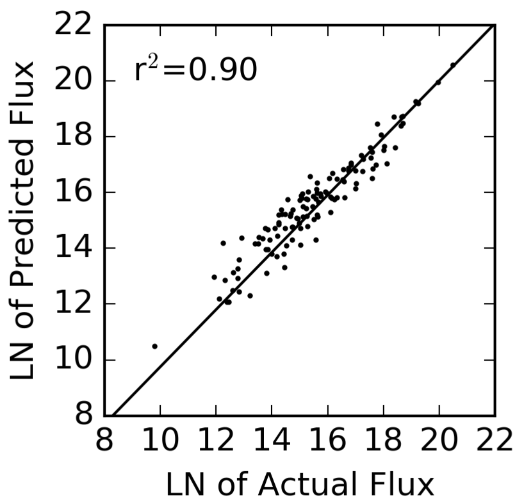

r²=0.90
LN of Predicted Flux
LN of Actual Flux
8
10
12
14
16
18
20
22

Figure 6.

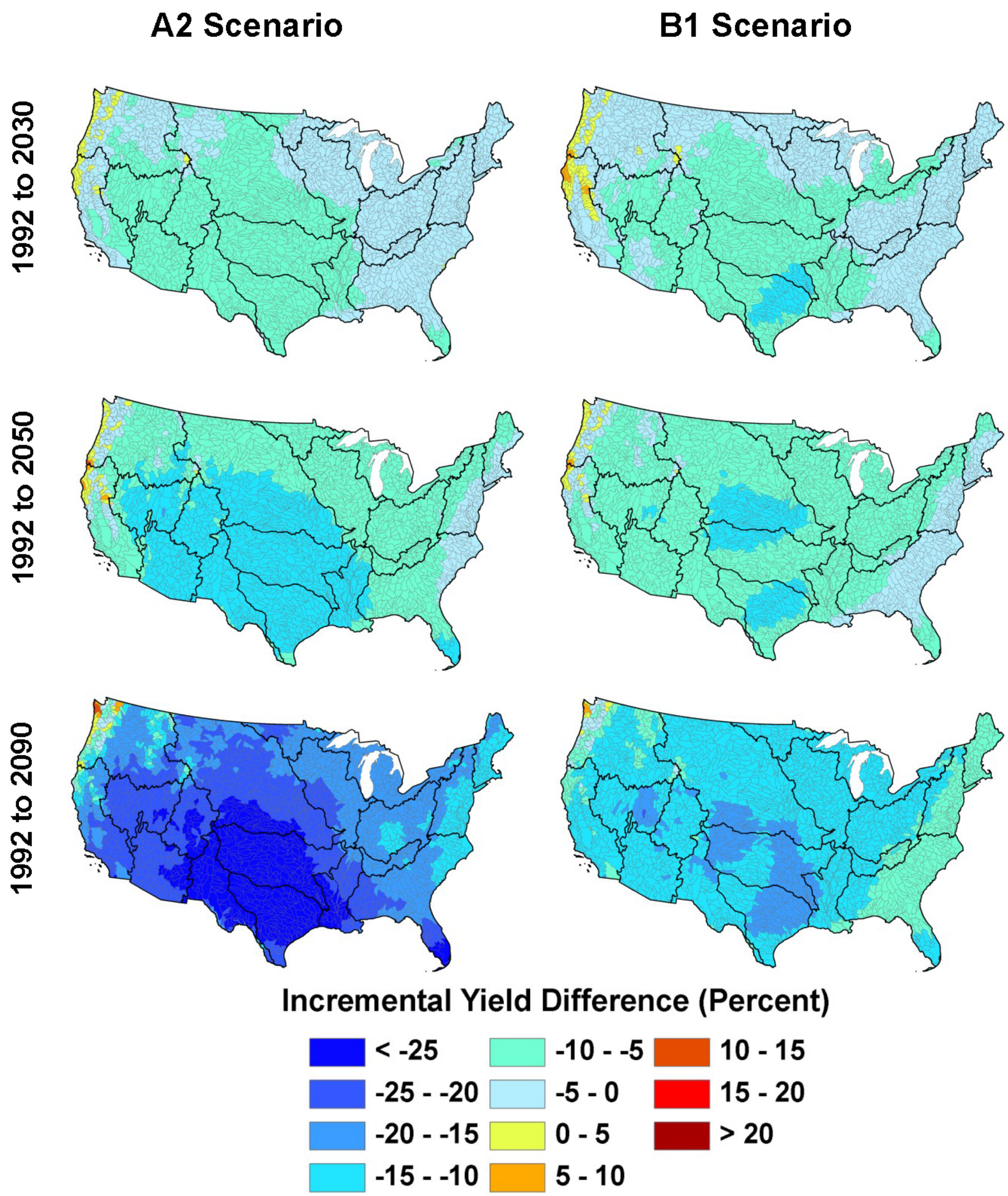

A2 Scenario
B1 Scenario
1992 to 2030
1992 to 2050
1992 to 2090
Incremental Yield Difference (Percent)
< -25
-25 - -20
-20 - -15
-15 - -10
-10 - -5
-5 - 0
0 - 5
5 - 10
10 - 15
15 - 20
> 20

Figure 7.

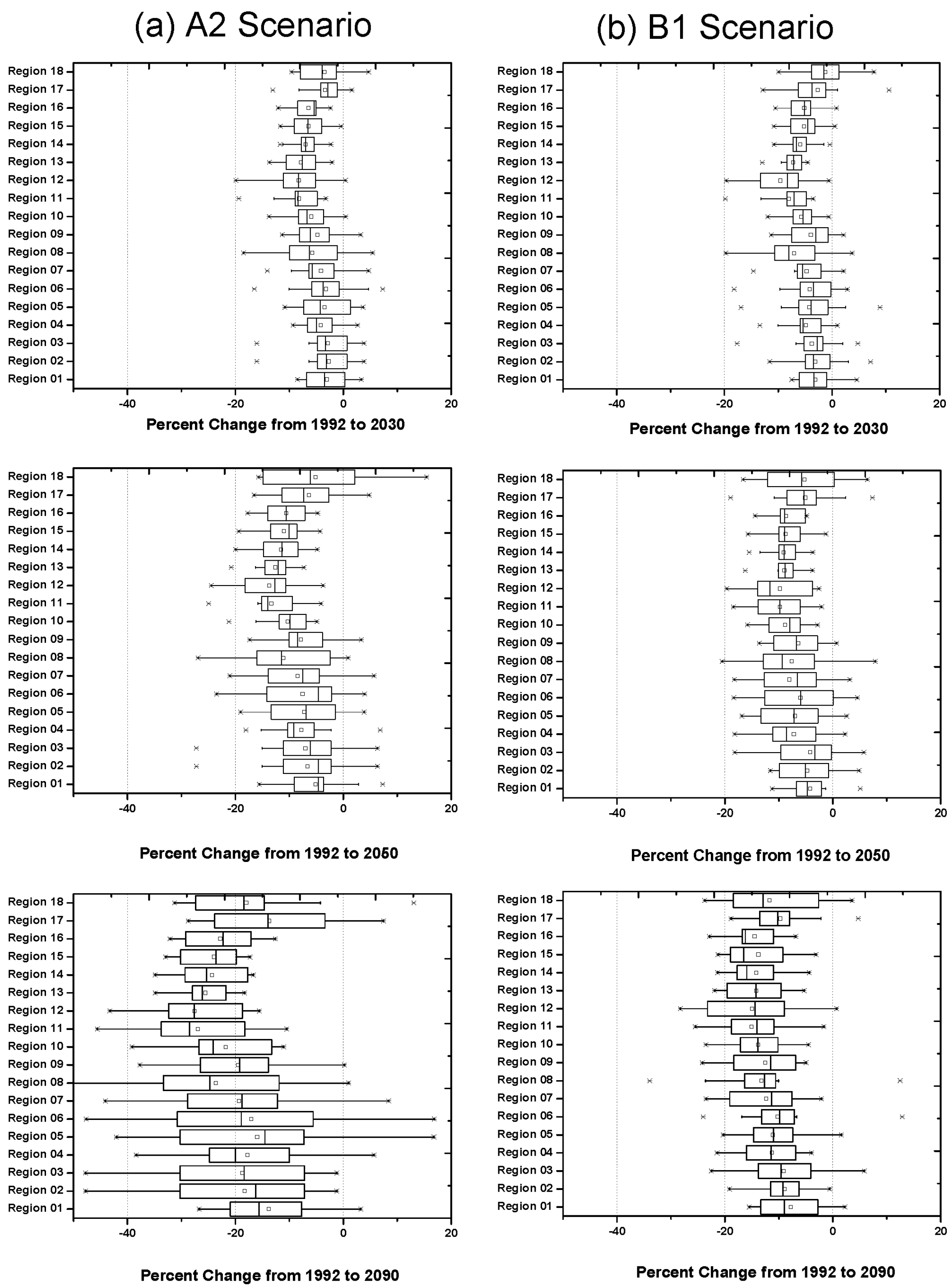

(a) A2 Scenario
(b) B1 Scenario
Region 18
Region 17
Region 16
Region 15
Region 14
Region 13
Region 12
Region 11
Region 10
Region 09
Region 08
Region 07
Region 06
Region 05
Region 04
Region 03
Region 02
Region 01
-40
-20
0
20
Percent Change from 1992 to 2030
Percent Change from 1992 to 2050
Percent Change from 1992 to 2090

Figure 8.

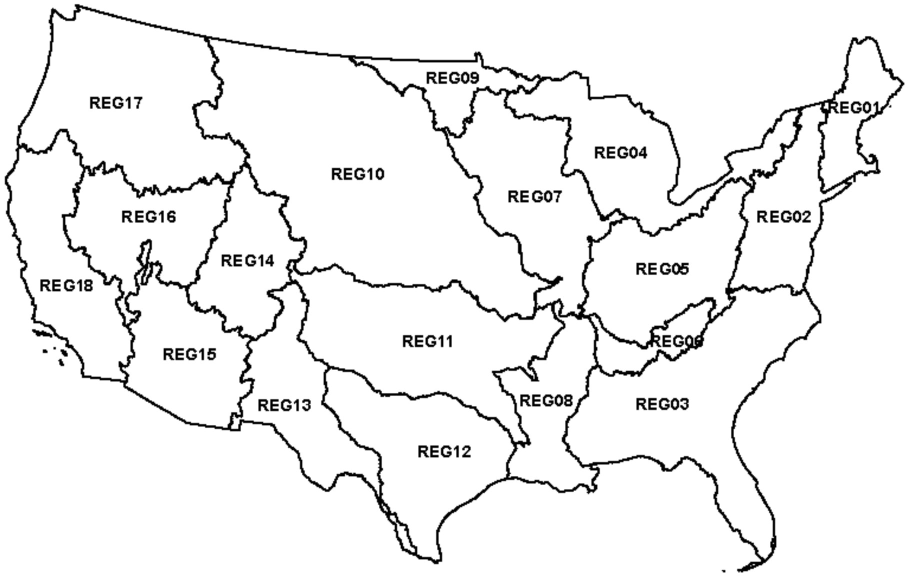
REG09
REG17
REG01
REG04
REG10
REG07
REG02
REG16
REG14
REG05
REG18
REG11
REG06
REG15
REG08
REG03
REG13
REG12

Figure 9.

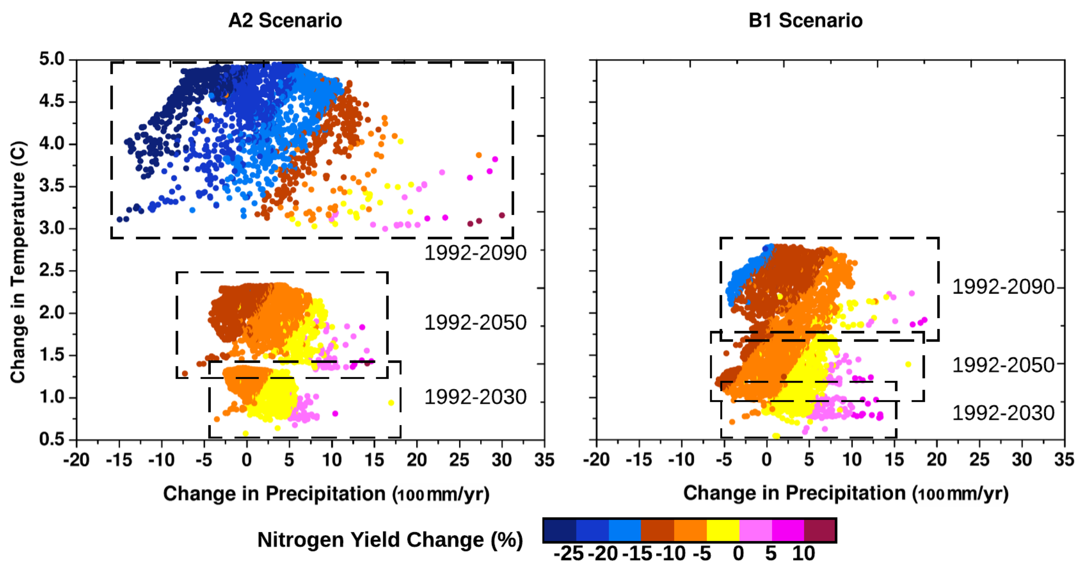
A2 Scenario
B1 Scenario
Change in Temperature (C)
5.0
4.5
4.0
3.5
3.0
2.5
2.0
1.5
1.0
0.5
1992-2090
1992-2050
1992-2030
-20 -15 -10 -5 0 5 10 15 20 25 30 35
Change in Precipitation (100 mm/yr)
Nitrogen Yield Change (%)
-25 -20 -15 -10 -5 0 5 10